Analysis and Correction of Echo Due to Mode Conversion in WC-281 Waveguide

Rod Walker

Abstract—**Testing of the antenna/waveguide systems of a long-haul, high-capacity microwave radio route showed unexpected high levels of group delay ripple. Initial analysis of these measurement results incorrectly indicated echo levels as high as 35 dB below wanted direct signal, as interpreted using a simplistic analysis technique which was later shown to be as much as 10–15 dB too pessimistic. Application of special Fourier analysis techniques to the test results subsequently showed that many of the cases of concern were in fact well within established system requirements. In other cases, it was found that installation of TE_{21} filters could readily be used to absorb the echo energy. The performance of the QAM radio used in this application was also characterized in terms of the residual BER tolerance to multiple echoes. The source of the echoes was isolated to TE_{21} mode generation within the WC-281 waveguide. To ensure the quality of new installations without the need for the application of filters, a method of pre-installation testing of waveguide sections to determine their individual moding levels was also established.**

I. Description of the Problem

A. General

A TE_{21} moding problem was encountered in WC-281 circular waveguide (inside diameter = 2.812 in.) during commissioning of a long-haul high-capacity digital microwave radio route. A large quantity of circular waveguide runs were used in this system, each typically 250 feet in length. Of these, a number exhibited TE_{11}/TE_{21} mode conversion, resulting in complex group delay patterns which indicated echo levels often in the order of 40–45 dB below dominant mode. Cases as high as 35 dB from wanted direct signal were initially calculated using a simplistic analysis technique which was subsequently shown to be as much as 10–15 dB too pessimistic. Initially it was feared that these levels of echo would degrade the digital radio residual bit-error-rate performance.

B. Historical Use of WC-281 Circular Waveguide

WC-281 circular waveguide has been in commercial use carrying 4, 6, 8, and 11 GHz telecommunications traffic since 1954. Use of this waveguide is a very cost-effective means of combining multiple frequency bands into one antenna feeder system with very low insertion loss.

All previously reported cases of TE_{21} mode conversion in the waveguide have been attributed to the flexible waveguide section used at the antenna, some waveguide transducers, antenna feed horns (to some extent) or to flange misalignment [1]–[3].

The antenna/waveguide arrangement used in this system made use of WC-281 waveguide to carry both 4- and 8-GHz digital microwave radio signals. Over each hop of the system, circular waveguide runs were used for the transmit, main receive, and one or two space-diversity antennas.

Manuscript received April 4, 1994; revised June 10, 1994.

The author is with Northern Telecom Canada Limited, Montréal, Canada H4S1K5

IEEE Log Number 9407450.

II. Measurement of Echo in the System

Testing of the antenna feeder system was performed through the use of the standard group delay test method which displays the differential phase response $\delta\phi/\delta\omega$ of a test signal swept over the radio channel bandwidth [4]. The echo level, relative to the wanted signal, is calculated from the product of the amplitude and the period of the sinusoidal display which results when a single echo is present (see Appendix). Multiple echoes of the magnitudes under consideration, add linearly in the display as multiple sinusoids.

A. The Group Delay Method

The basic principles of the group delay (differential phase) method are as follows. (See Appendix for a complete proof.)

A frequency-modulated signal $D(t)$ of the form shown here, per reference [5], (normalized) is generated by the Microwave Link Analyser (MLA) test set:

$$D(t) = \cos\left[\omega_c t + \int \Delta\omega \sin(pt)\, dt\right] \tag{1}$$

$$= \cos[\omega_c t + \Delta\omega/p \cos(pt)];$$

$$p = \text{search frequency} \tag{2}$$

$$= \cos[\omega_c t + S(t)];$$

$$S(t) = \Delta\omega/p \cos(pt). \tag{3}$$

In the group delay test, signal $D(t)$ is sent through the system and is received at the other end of the hop, where it is demodulated. Echoes generated in the system are added to the direct received signal and the total received signal appears as:

$$R(t) = D(t) + \sum E_i(t) \tag{4}$$

$$R(t) = \cos(\omega_c t + S(t)) + \sum a_i \cos(\omega_c(t - \tau_i) + S(t - \tau_i) + \phi_i) \tag{5}$$

where a_i and τ_i are the relative amplitude and delay of the ith echo signal. ϕ_i is a fixed phase change for each echo due to reflection. The FM signal $R(t)$ is demodulated at the

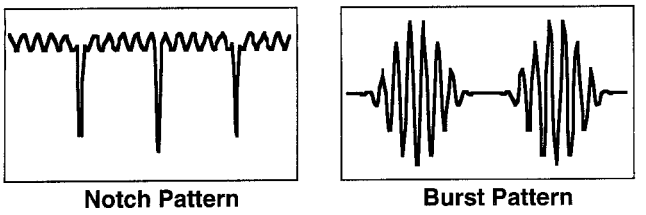

Fig. 1. Complex group delay patterns observed.

receiver and the receive MLA then displays the differential phase $d\varphi/dp$ of the demodulated signal $Z(t)$,

$$d\varphi/dp \approx \sum a_i\tau_i[\sin(p\tau_i)/(p\tau_i)]\cos(\omega_c\tau_i + \phi_i) \quad (6)$$

as the carrier frequency ω_c is swept across the band. Each echo component of delay τ_i adds linearly as a sinusoid of period $1/\tau_i$ and amplitude $a_i\tau_i[\sin(p\tau_i)/(p\tau_i)]$.

The desired relative echo amplitude ai for each echo component is calculated as:

$$a_i = (\text{Period}) * (\text{Displayed Amplitude}) * [\sin(p\tau_i)/(p\tau_i)]^{-1}. \quad (7)$$

Conversion to dB relative to direct signal amplitude is then:

$$A_i(\text{dB}) = 66 - 20\log\{(\text{Period (MHz)} * \text{Peak-Peak Amplitude (ns)} * [\sin(p\tau_i)/(p\tau_i)]^{-1}\} \quad (8)$$

where the value 66 results from the use of MHz and ns units, and peak-to-peak amplitude.

B. Modeling of the Group Delay Differential Phase Echo Patterns

1) Observed Field Patterns: In the system under study, two types of complex patterns were frequently observed similar to those shown in Fig. 1. Initial simplistic field analysis treated these patterns as sinusoids and applied the formula of (8) using the periodicity of the patterns and their worst case amplitudes. It was later shown that the true total effective echo was typically 6 dB lower than the level calculated simplistically, while cases as inaccurate as 15 dB were observed.

To determine the sinusoidal (i.e. individual echo) components of these patterns, a Fourier Series model was constructed. From the derived components of the model the total effective echo could then be calculated.

2) The Repeating Notch Pattern Model: The repeating notch pattern was modeled as a repeating single truncated cosine pulse as shown in Fig. 2. The cosine model best approximated the entire range of observed field patterns, which in practice were noted to merge into a single sinusoid as the fundamental echo distance (due to the length of the moding circular waveguide run) became longer.

The Fourier Series for this model is the following:

$$\delta\phi/\delta\omega = -A\tau/2T - \sum_{n=1\to\infty} F(A,n,\tau,T) * \cos(2n\pi f/T) \quad (9)$$

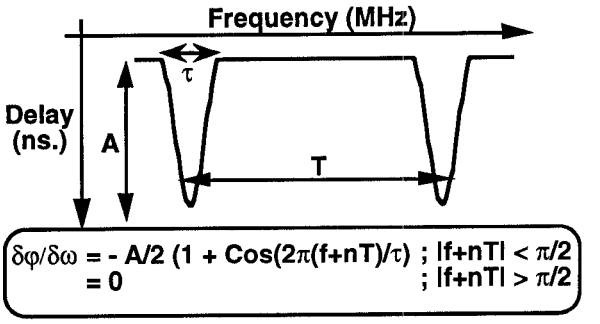

Fig. 2. Repeating notch pattern model.

where

$$F(A,n,\tau,T) = (A/n\tau) * \sin(n\pi\tau/T) + (A\tau/(2\pi T - 2n\pi\tau)) * \sin\pi(1 - n\tau/T) + (A\tau/(2\pi T + 2n\pi\tau)) * \sin\pi(1 + n\tau/T) \quad (10)$$

Using (8), calculation of the echo in each term of the series of:

$$\text{Frequency} = (n/T) \quad (11)$$

and

$$\text{Peak-to-Peak Amplitude} = 2 * F(A,n,\tau,T) \quad (12)$$

is easily done. The echo in each sinusoidal term is then:

$$S/E(n) = 66 - 20\log\{[T/n] * 2 * F(A,n,\tau,T) * [\sin(pn/T)/(pn/T)]^{-1}\}. \quad (13)$$

3) The Repeating Burst Pattern Model: Modeling of the repeating burst pattern was easily done by applying a high-frequency amplitude modulation (with respect to the pulse width τ) to the repeating notch series. The pulse cosine shape employed in the model conformed well with the shape of the measured bursts.

The Fourier Series for this model was therefore:

$$\begin{aligned}\delta\phi/\delta\omega &= -A\tau/2T\cos(\omega\tau_{am}) - \sum_{n=1\to\infty} F(A,n,\tau,T) * \cos(2n\pi f/T) * \cos(\omega\tau_{am}) \\ &= -A\tau/2T\cos(\omega\tau_{am}) - \sum_{n=1\to\infty} 0.5 * F(A,n,\tau,T) * \cos(2n\pi f/T + \omega\tau_{am}) - \sum_{n=1\to\infty} 0.5 * F(A,n,\tau,T) * \cos(2n\pi f/T - \omega\tau_{am}).\end{aligned} \quad (14)$$

Calculation of the echo in each term of this series is done as above. The echo in each sinusoidal term (with the exception of the AM modulated dc term) is then:

$$S/E(n) = 66 - 20\log([n/2T \pm \tau_{am}] * F(A,n,\tau,T) * [\sin(p\{n/T \pm \tau_{am}\})/(p\{n/T \pm \tau_{am}\})]^{-1}) \quad (15)$$

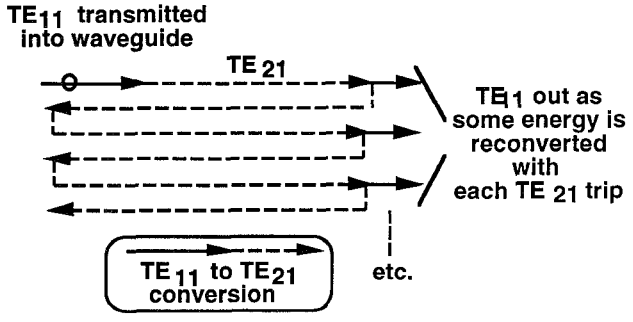

Fig. 3. Trapped TE_{21} signal echoes-notch effect.

4) Physical Significance of the Fourier Model: The validity of the model in describing the physical phenomenon was established through both an understanding of the mode trapping phenomenon occurring in the waveguide, and through correlation of the echo delays of the sinusoid terms in the series with those of echoes in the waveguide systems.

When broadband moding is created by a fault in the waveguide, the resulting signal echo travels a large number of times up and down the waveguide (due to constrictive sections at each end which do not pass the TE_{21} mode) [6]. Each time it passes a reconversion point due to a physical anomaly, some small portion of its energy is reconverted to the wanted TE_{11} mode and is transmitted out of the system as a delayed signal. Consequently, a series of signals, each one delayed by one additional trip up and down the system is generated. The pattern of each signal in the group delay display is a cosine function (i.e. $\delta\phi/\delta\omega = An\tau\cos(\omega n\tau)$). The measured group delay display then, is a series of terms with the same frequency characteristics as the Fourier Series. To verify this explanation, the echo delays associated with the periods of the components of the group delay model, were compared with good results against the expected propagation delays of TE_{21} modes in the waveguides being tested.

The notch pattern was found to be caused by propagation delays over the full length of the waveguide as illustrated in Fig. 3. Notches typically occurred on short runs where multiple reconversion points are less likely and so full round-trip propagation of the mode energy in the waveguide occurs.

The "multiple echo burst" analysis indicated that the pattern was generated by two series of TE_{21} modes, whose delay periods differed from one series to the next by a value due to travelling a difference of two to three waveguide section lengths (25–37.5 ft.), theoretically resulting from two reconversion points spaced at this distance, as illustrated in Fig. 4. Where more reconversion points exist more series of varying differences in delay periods should theoretically result. It was found however, that almost any pattern could be closely approximated using the two series model described above, so this simpler model was used.

A software tool was developed from the Fourier equations which, with careful adjustment of parameters, allowed very accurate duplication of the group delay patterns observed in the system.

5) Models Based Upon the Physical Phenomenon: A computer simulation model was also constructed on the basis

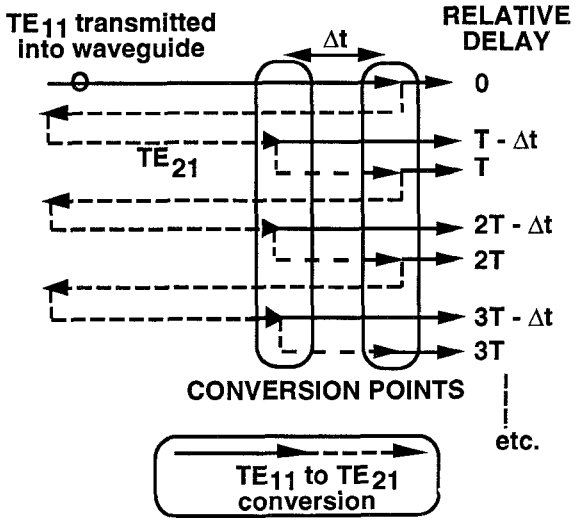

Fig. 4. Trapped TE_{21} signal echoes-burst effect.

of the physical description given above. In this model it was assumed that each time a mode reconversion occurred the TE_{21} signal suffered a fixed conversion loss r. The non-converted remaining TE_{21} echo energy was therefore subsequently reduced by the energy transferred to TE_{11} mode by reconversion.

In this description, the first time a reconversion occurs, the reconverted mode energy $(TE_{21} -> TE_{11})_1$ and the first non-reconverted remaining $(TE_{21})_1$ energy are expressed as:

$$\begin{aligned}&\text{Reconverted } (TE_{21} \rightarrow TE_{11})_1 \\ &\quad = A * r * \cos[2\pi f(\tau + \Delta\tau + t)] \\ &\text{Non-Reconverted } (TE_{21})_1 \\ &\quad = A * (1 - r) * \cos[2\pi f(\tau + \Delta\tau + t)] \end{aligned} \tag{16}$$

where r is the fixed reconversion loss, τ is the incremental delay suffered by each bounce, and $\Delta\tau$ is a possible fixed delay common to all echoes.

By extension, the nth reconverted mode $(TE_{21} \rightarrow TE_{11})n$ and the nth non-reconverted remaining $(TE_{21})n$ energy are expressed as:

$$\begin{aligned}&\text{Reconverted } (TE_{21} \rightarrow TE_{11})_n \\ &\quad = A * (1 - r)^{n-1} * r * \cos[2\pi f(n\tau + \Delta\tau + t)] \\ &\text{Non-Reconverted } (TE_{21})_n \\ &\quad = A * (1 - r)^{n} * \cos[2\pi f(n\tau + \Delta\tau + t)]. \end{aligned} \tag{17}$$

The resultant group delay $\delta\phi/\delta\omega$ expression using this model is therefore:

$$\begin{aligned}\delta\phi/\delta\omega = &\sum_{n=1\rightarrow\infty} [A * (1 - r)^{n-1} * r * (n\tau)] \\ &* [\sin(pn\tau)/(pn\tau)] \\ &* \cos[2\pi f(n\tau + \Delta\tau = \phi)]. \end{aligned} \tag{18}$$

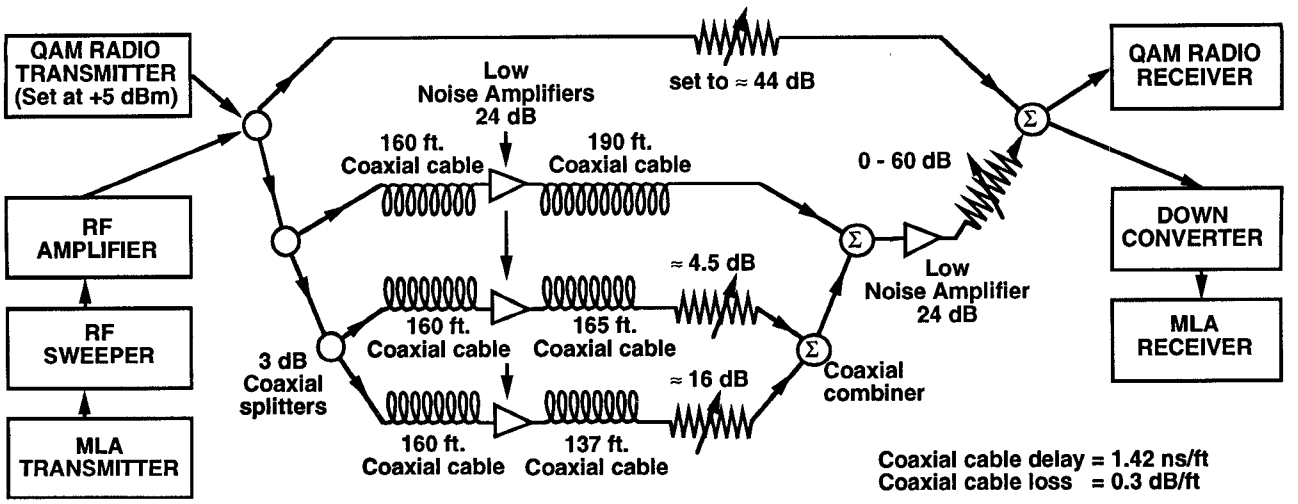

Fig. 5. Coaxial test setup for repeating burst.

The echo in each sinusoid term can be calculated as

$$S/E(n) = 66 - 20\log\{[A*(1-r)^{n-1}*r*(n\tau)] * [\sin(pn\tau)/(pn\tau)]*(1/n\tau)\} \quad (19)$$

Simulations using this description resulted in very good pattern reproduction, and total "effective" echo calculations (to be discussed below) within 1 dB of those generated from the Fourier models described above. This result further substantiated the validity of the Fourier model.

6) Multiple Echo Addition Rule from Radio Performance Testing: Experimental laboratory work performed on the QAM digital radio confirmed both the final echo requirement of 49 dB to meet the radio residual BER specification of 10^{-13}, as well as the method of calculation of the total effective degradation where multiple echoes are present.

The performance of the QAM radio was measured in the presence of both a single echo interferer and several complex echo patterns similar to those observed in the waveguide systems. The complex echoes were generated with coaxial delay lines under controlled laboratory conditions using echo delays and amplitudes calculated from the Fourier model, using the set-up shown in Fig. 5 (burst case shown). The appropriate coaxial lengths were calculated from the inverse of the frequencies given in equation (11) and (as part of) (14). For the burst case shown in Fig. 6, the delays of 498 ns = 1/2.01 MHz, 461 ns = 1/2.17 MHz, and 422 ns = 1/2.37 MHz, result from setting T = 26 MHz, τ = 20 MHz, and τ_{am} = 458 ns in those equations. The resulting cable lengths of 350 ft., 325 ft. and 297 ft. were calculated using a cable delay of 1.42 ns/ft. The associated relative levels of 1.0 unit of amplitude (2.01 and 2.17 MHz echoes) and 0.74 units of amplitude (2.37 MHz echo) were achieved using attenuators. Amplifiers were required to maintain the signal levels within the input range of the radio receiver.

The measured BER was then plotted against both the strength of the single echo and that of the complex echo ensemble as calculated according to the following addition rules:

a) Coherent Voltage Addition:

$$\text{E(total)} = \sum_{i=1\to N} e_i \quad (20)$$

b) RSS (Root of Sum of Squares) Addition

$$\text{E(total)} = \left(\sum_{i=1\to N} e_i^2\right)^{1/2} \quad (21)$$

c) 3/2 Power Law Addition:

$$\text{E(total)} = \left(\sum_{i=1\to N} e_i^{3/2}\right)^{2/3} \quad (22)$$

d) Simplistic Method:

$$\text{E(total)} = \text{Maximum } P\text{-}P \text{ Amplitude} * \text{Period} \quad (23)$$

(e_i is the level of the ith echo component.)

Direct comparison of the calculated strength of the echo ensemble to that of the single echo permitted determination of the most accurate addition rule. The rule ultimately selected was based upon obtaining the minimum difference in resulting BER for a given signal to echo ratio over a range of signal to echo values. (Those cases where at least one component fell within the radio ATDE (Adaptive Time Domain Equalizer) range were not taken into account in the determination of the rule due to the obvious alteration of the sum by the ATDE influence).

Due to the signal losses imposed through the use of coaxial delay lines, a limited, but very representative, set of test cases could be constructed. Two burst patterns were simulated where all components were outside of the ATDE range. Two other cases, one notch pattern, and one less well defined pattern, were also constructed where at least one component fell within the ATDE range. In the latter cases the radio performance was far better than in the former cases. A number of differing levels of additional interfering noise were also introduced to raise the value of the echo free residual FEC (Forward Error Correction) count which was used as an indirect measure of

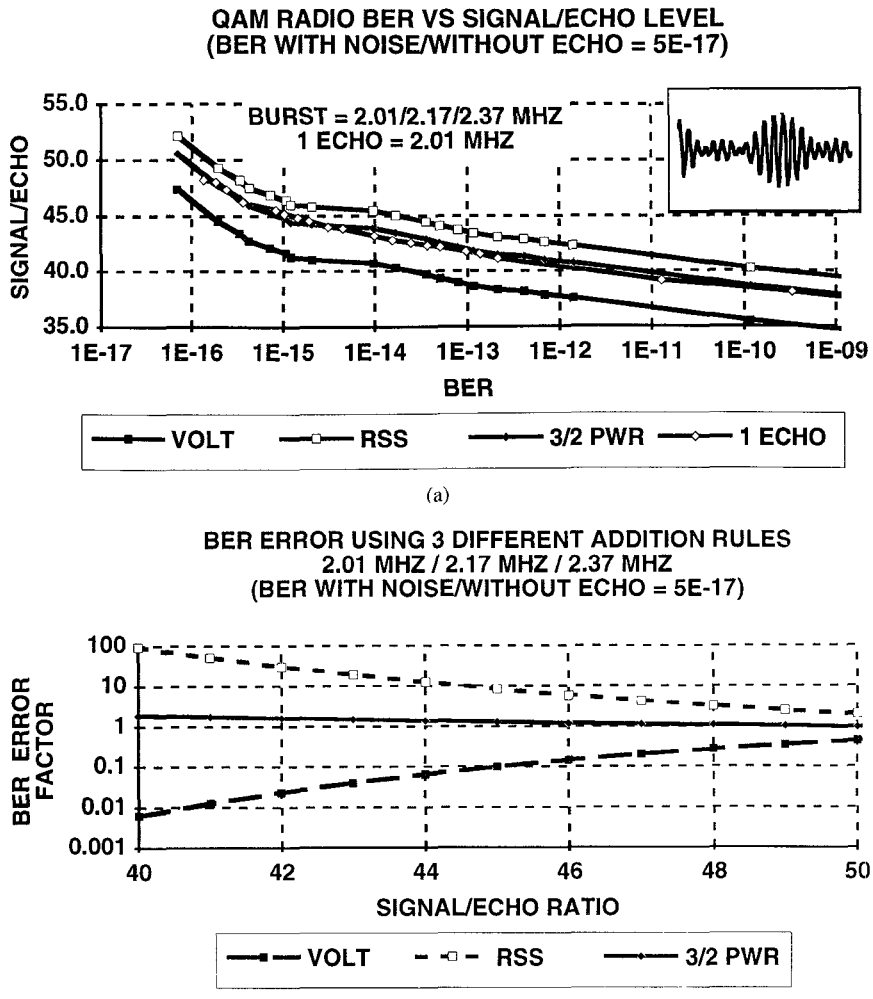

Fig. 6. (a) QAM radio BER with 2.01/2.17/2.37 MHz echo components, (b) BER error with 2.01/2.17/2.37 MHz echo components.

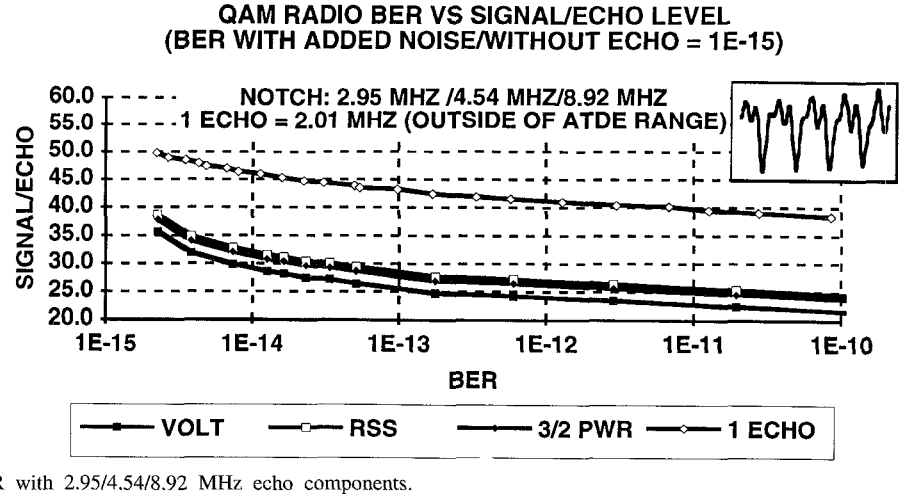

Fig. 7. QAM radio BER with 2.95/4.54/8.92 MHz echo components.

bit error rate. This represented expected field conditions where other noise sources could be present.

Figs. 6 and 7 show the measured residual BER of two of the test cases (with added noise) as a function of a single echo, and of the complex echo ensembles.

The error in expected residual BER for the complex echo patterns using the three calculation methods for the burst case is also shown in Fig. 6(b). The use of the 3/2 power law addition rule gave the closest estimation of the BER, to within a factor of 1.9, while the voltage, simplistic and RSS addition

methods resulted in errors of one to two orders of magnitude for the BERs of interest and the patterns generated in the tests. Note that the simplistic method discussed above gave results to within 0.5 dB of those of the voltage addition rule.

The ATDE performance was clearly evident in the high levels of echo which could be tolerated in the two cases with short echo delays. As a result, the 3/2 power law addition rule was found to be invalid for such short delay echoes, as shown in Fig. 7.

While testing of other QAM radios was not undertaken, it is believed that the same addition rule would most likely be applicable as the same modulation process is used.

III. Determination of the Moding Source

Following extensive investigation it was shown that the mode conversion was occuring within the WC-281 waveguide. Replacement of the waveguide with sections manufactured in the 1950's eliminated the moding. The copper tubing associated with all previously examined pieces had exhibited a set of rings of light on the inside walls, suggesting a varying diameter. The 1950's vintage waveguide sections did not have this characteristic.

A large quantity of such 1950's vintage waveguide sections was subsequently installed with excellent success. It has since been reported by one supplier however, that notable levels of mode conversion have been observed in a number of waveguide sections from that period.

This problem of mode generation was brought to the attention of the copper-tubing manufacturer and further mechanical study has been performed. Unfortunately no correlation to dates of manufacture or batches has been established. (A paper to be published entitled "Multimoding in WC-281 Circular Waveguide used in Horn Antenna Feeder Systems" by Mr. P.A. Nwafor of Stentor discusses the results of a mechanical study into the manufacturing process which resulted in the mode conversion.)

IV. Waveguide Screening Process

A. Calculation of Acceptable Moding Level of Single Sections

To ensure that all installed waveguide sections be free of mode conversion, a procurement specification as well as a method of "bench" measurement of single waveguide 12.5-foot sections were established.

The acceptable level of mode generation of any one section of waveguide is based upon the proportion of the total allowable system echo level each contributor in the system is allotted. The total tolerable echo level in the system over the hop was set at 49 dB below wanted signal.

A theoretical analysis of the expected worst-case echo induced from return-loss of the system components, indicated that a level of 53 dB below wanted signal was attainable. Using the "3/2 power law" method of calculation discussed above, it was determined that an additional echo due to moding of 53 dB could then be tolerated. Calculation of two runs of eighteen (18) tandem waveguide sections, (which represented a typical transmit/receive combination of runs in the system),

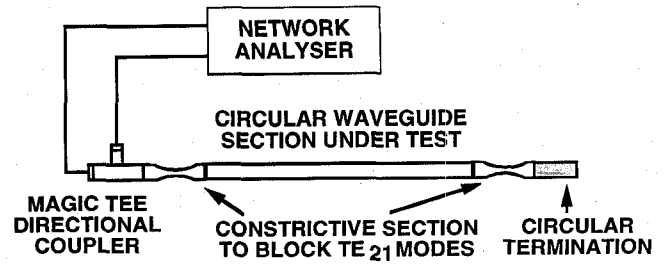

Fig. 8. Testing of circular waveguide sections.

with approximately 50% of the sections generating echoes levels due to moding of 70 dB, resulted in a total moding echo level of 53 dB. When combined with the return-loss echo the maximum allowable value of 49 dB is attained. In practice it was found that 40–50% of the waveguide sections on runs where these group delay patterns were observed exhibited mode conversion.

It was on the basis of this calculation that the mode conversion requirement of 70 dB per waveguide section was established.

B. Measurement Technique to Characterize the Waveguide Prior to Installation

Testing of single sections of waveguide prior to installation, to determine their individual moding levels, was performed using a return-loss sweep of the waveguide in a mode trapping configuration. This technique was adopted for single section tests in place of the more accurate group delay test, as the latter relies on calculation of echo from the displayed pattern period. On a single section of waveguide this period is greater than 20 MHz due to the short delay time. The group delay test equipment was designed for narrowband testing (unlike the return-loss test equipment) and as such was inappropriate for testing of such short delay ripples.

In the return-loss test setup, the waveguide is terminated at one end with a constrictive waveguide section and a circular termination, while the other end is connected through a second constrictive section to a magic tee as shown in Fig. 8. In this way, generated TE_{21} modes are trapped and will travel up and down the waveguide section until they reconvert to the dominant TE_{11} mode and then escape [6]. This phenomenon is identical to that which produces mode-spikes in the group delay display.

In this test, these modes result in a bipolar return-loss spike where the TE_{21} energy reconverted to TE_{11} (which is ultimately measured) adds to the normal TE_{11} return-loss energy which is always present. The resulting return-loss plot is as shown in Fig. 9.

At the points in the plot at which the spike occurs it is assumed for the purposes of this calculation that the mode energy echo terms all add in phase. This "is realized by making the . . . pipe run an integral number of half wavelengths," per reference [6] where the analysis was performed with WC-205 waveguide. As coherent phase addition does not generally occur in most cases, this assumption results in an inaccurate calculation, but one which provides a simplistic field analysis method. Numerical analysis of mode-spike patterns created from the physical model of delayed echoes showed that this

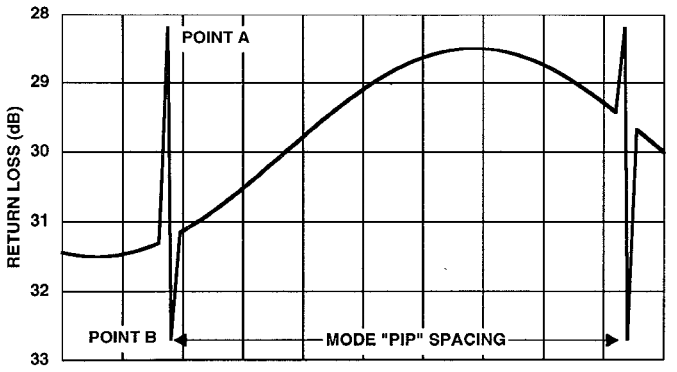

Fig. 9. Mode spikes in the return-loss plot.

assumption can result in 6 to 12 dB higher estimated mode levels than actually exist using the "3/2 power law" method. For this reason, using this method, the requirement of 70 dB was lowered to 65 dB, which was much more easily achieved.

The mode level analysis from this effect is as follows:

At points A and B in Fig. 9, the dominant mode, defined as D (return-loss energy) and the unwanted mode energy M add as:

$$A = 20 \log \left(D + \sum (M)\right); \qquad A \text{ in dB} \tag{24}$$

$$B = 20 \log \left(D - \sum (M)\right); \qquad B \text{ in dB}. \tag{25}$$

Knowing the value of A and B from the measurement, the mode level, relative to the inserted signal is determined as:

$$20 \log \left(\sum (M)\right) = 20 \log [(1/2)(10^{(A/20)} - 10^{(B/20)})]; \quad A, B < 0. \tag{26}$$

In order to maintain the desired accuracy, the circular termination used had a minimum return-loss of 50 dB, and the magic tee a minimum directivity of 45 dB.

Calibration was performed in a "back to back" configuration without the inserted circular waveguide, to ensure that the test set-up generated a maximum 80 dB moding level. This requirement was achievable only through the use of transducers specially tuned for minimal mode conversion.

Each waveguide piece under test was then verified against the requirement specification of 65 dB. The entire band of interest was swept using a 130-MHz sweep width with an resolution of 1 dB per division.

From this measurement, the quality of the test equipment and the waveguide sections could be readily evaluated.

V. Constrictive and Suppressive Filter Solutions

Removal of the constrictive waveguide filter section and replacement with a straight WC-281 piece was always the first step in attempting to eliminate the moding in the system. This allowed the mode energy to pass to the antenna without reconversion to TE_{11} and be radiated as weak sidelobe patterns. This solution worked however only in a minimum number of cases. The echo was generally reconverted to TE_{11} prior to being radiated and therefore became a short delay echo (due to only one trip through the waveguide at the slower TE_{21} velocity) added to the undelayed wanted signal. The echo level was usually not significantly reduced and in this case this simple solution was deemed unsatisfactory.

A TE_{21} suppressive filter developed by the waveguide supplier to resolve this difficulty, was found to be very effective in reducing levels of echo typically by 20 dB (two units in tandem) when placed in the waveguide run. This filter is designed to terminate TE_{21} modes while allowing all other modes to pass with very little insertion loss, typically 0.1 dB (two units in tandem). The filters were optimized for the best combination of XPD (Cross Polarization Discrimination) and mode suppression for both polarizations. This application was successful and was used extensively in the system where echo levels exceeded specifications.

The filter solutions were less effective on long waveguide runs due to mode conversion and reconversion prior to the energy encountering the suppression filter or the antenna. In one test case, placement of a filter at the center of the run was found to be most effective.

Appendix
Proof of the Group Delay Method of Echo Measurement

The direct signal generated by the Microwave Link Analyser (MLA) transmitter test set is of the form (normalized):

$$D(t) = \cos\left(\omega_c t + \int \Delta\omega \sin(pt)\, dt\right) \tag{A.1}$$

$$= \cos(\omega_c t + \Delta\omega/p \cos(pt));$$

$$p = \text{search frequency} \tag{A.2}$$

$$= \cos(\omega_c t + S(t)); \qquad S(t) = \Delta\omega/p \cos(pt). \tag{A.3}$$

Echoes generated in the system are of the form

$$E_i(t) = a_i \cos(\omega_c(t - \tau_i) + S(t - \tau_i) + \phi_i). \tag{A.4}$$

The total receive signal including echoes is therefore

$$R(t) = D(t) \sum E_i(t) \tag{A.5}$$

$$R(t) = \cos(\omega_c t + S(t)) + \sum a_i \cos(\omega_c(t - \tau_i) + S(t - \tau_i) + \phi_i) \tag{A.6}$$

$$R(t) = \cos(\omega_c t + S(t)) \left[1 + \sum a_i \cos \cdot (\omega_c \tau_i + S(t) - S(t - \tau_i) + \phi_i)\right] \tag{A.7}$$

$$+ \sin(\omega_c t + S(t)) \cdot \left[\sum a_i \sin(\omega_c \tau_i + S(t) - S(t - \tau_i) - \phi_i)\right] \tag{A.8}$$

$$R(t) = |R(t)| * \cos(\omega_c t + S(t) + \Phi) \tag{A.9}$$

and

$$\Phi = \tan^{-1}\left[\sum a_i \sin(\omega_c \tau_i + S(t) - S(t - \tau_i) - \phi_i) \Big/ \left[1 + \sum a_i \cos(\omega_c \tau_i + S(t) - S(t - \tau_i) + \phi_i)\right]\right] \tag{A.10}$$

and

$$\Phi \approx \sum a_i \sin(\omega_c \tau_i + S(t) - S(t-\tau_i) - \phi_i). \quad \text{(A.11)}$$

The receive signal is applied to an FM demodulator to recover the search signal.

$$R(t) \rightarrow \text{FM demodulator} \rightarrow Z(t)$$

where

$$Z(t) = \delta(\omega_c t + S(t) + \Phi)/\delta t \quad \text{(A.12)}$$

$$Z(t) = \omega_c + \delta S(t)/\delta t + \delta\Big(\sum a_i \sin(\omega_c \tau_i + S(t) - S(t-\tau_i) - \phi_i)\Big)\Big/\delta t. \quad \text{(A.13)}$$

This can be simplified by noting that

$$S(t) - S(t-\tau_i) = \Delta\omega/p \cos(pt) - \Delta\omega/p \cos(p(t-\tau_i)) \quad \text{(A.14)}$$

$$= -2\Delta\omega/p \sin(p\tau_i/2) \sin(pt - p\tau_i/2) \quad \text{(A.15)}$$

$$Z(t) = \omega_c - \Delta\omega \sin(pt) - \sum a_i \cos(\omega_c \tau_i - 2\Delta\omega/p \sin(p\tau_i/2) \cdot \sin(pt - p\tau_i/2) - \phi_i)) * (2\Delta\omega \sin(p\tau_i/2) \cdot \cos(pt - p\tau_i/2)) \quad \text{(A.16)}$$

Dropping the constant term ω_c,

$$Z(t) = -\Delta\omega \sin(pt) - 2\Delta\omega \cdot \sum a_i \sin(p\tau_i/2) \cos(pt - p\tau_i/2) * \cos(\omega_c \tau_i - 2\Delta\omega/p \sin(p\tau_i/2) \cdot \sin(pt - p\tau_i/2) + \phi_i)). \quad \text{(A.17)}$$

Some simplifications can be made by noting typical values of the terms as follows:

$$\Delta\omega = 140,000 * 2 * \pi = (0.88)10^6$$
$$p = (83,000 * 2 * \pi) = 5.21 * 10^5$$
$$\tau_i = 10^{-6}$$
$$\omega_c = 4.7 * 10^9 * 2 * \pi = 2.95 * 10^{10} \quad \text{(A.18)}$$

Therefore

$$p\tau_i/2 = 0.26 \qquad 2\Delta\omega/p = 3.37$$
$$\omega_c \tau_i = 2.95 * 10^4. \quad \text{(A.19)}$$

Since $\omega_c \tau_i \gg 2\Delta\omega/p$ and since both $\Delta\omega$ and p are constants while ω_c is swept across the band of interest, then the expression may be approximated by:

$$Z(t) \approx -\Delta\omega \sin(pt) - 2\Delta\omega \sum a_i \sin(p\tau_i/2) \cdot \cos(pt - p\tau_i/2) \cos(\omega_c \tau_i + \phi_i)). \quad \text{(A.20)}$$

Also since $p\tau_i/2 = 0.26$ using the same typical values, $\sin(p\tau_i/2) = p\tau_i/2$. Therefore:

$$Z(t) \approx -\Delta\omega \sin(pt) - \Delta\omega p \sum a_i \tau_i \cos(pt - p\tau_i/2) \cdot \cos(\omega_c \tau_i + \phi_i)) \quad \text{(A.21)}$$

and through trigonometric manipulation

$$Z(t) \approx \sin(pt)\Big[-\Delta\omega - \Delta\omega p \sum a_i \tau_i \cdot \sin(p\tau_i/2) \cos(\omega_c \tau_i + \phi_i))\Big] + \cos(pt)\Big[-\Delta\omega p \sum a_i \tau_i \cdot \cos(p\tau_i/2) \cos(\omega_c \tau_i + \phi_i))\Big] \quad \text{(A.22)}$$

$$Z(t) = |Z(t)| * \sin(pt + \varphi) \quad \text{(A.23)}$$

where

$$\varphi = \tan^{-1}\Big\{\Big[-\Delta\omega p \sum a_i \tau_i \cos(p\tau_i/2) \cdot \cos(\omega_c \tau_i + \phi_i))\Big]\Big/\Big[-\Delta\omega - \Delta\omega p \sum a_i \tau_i \cdot \sin(p\tau_i/2) \cos(\omega_c \tau_i + \phi_i))\Big]\Big\} \quad \text{(A.24)}$$

and since $pa_i\tau_i = 0.0052$, using the same typical values

$$\varphi \approx \tan^{-1}\Big[p \sum a_i \tau_i \cos(p\tau_i/2) \cos(\omega_c \tau_i + \phi_i))\Big] \quad \text{(A.25)}$$

$$\approx \Big[p \sum a_i \tau_i \cos(p\tau_i/2) \cos(\omega_c \tau_i + \phi_i))\Big] \quad \text{(A.26)}$$

$$d\varphi/dp = \Big[\sum a_i \tau_i \cos(p\tau_i/2) \cos(\omega_c \tau_i + \phi_i))\Big] + p \sum a_i \tau_i^2/2 \sin(p\tau_i/2) \cos(\omega_c \tau_i + \phi_i))\Big] \quad \text{(A.27)}$$

and since $a_i\tau_i > pa_i\tau_i^2/2$ (i.e typically $p\tau_i/2 = 0.26$) another approximation may be made. [Note that numerical analysis using this approximation, and all others in this proof, of the calculated levels of both single echoes and complex echo ensembles was performed. A maximum total effective echo level error of 2 dB (lower total effective echo level) was calculated.]

$$d\varphi/dp \approx \Big[\sum a_i \tau_i \cos(p\tau_i/2) \cos(\omega_c \tau_i + \phi_i)\Big]. \quad \text{(A.28)}$$

Using the approximation $\sin(p\tau_i/2) = p\tau_i/2$ and the trigonometric relationship:

$$\sin(p\tau_i/2) \cos(p\tau_i/2) = 1/2[\sin(p\tau_i/2 - p\tau_i/2) + \sin(p\tau_i/2 + p\tau_i/2)] \quad \text{(A.29)}$$

$$d\varphi/dp \approx \sum a_i \tau_i [\sin(p\tau_i)/(p\tau_i)] \cos(\omega_c \tau_i + \phi_i)). \quad \text{(A.30)}$$

This is the traditional differential phase response expression used to calculate the echo level a_i.

VII. Conclusion

The predominant TE_{21} moding problem was shown to be caused by the copper tubing used in some WC-281 circular waveguide. No correlation to date of manufacture or batch has been established. The mechanical anomaly causing this problem was referred to the tubing manufacturer. Recent preliminary feedback from suppliers indicates that the manufacturing fault which caused the mode conversion has been identified and corrected.

A method of pre-installation testing of waveguide sections to determine their individual moding levels was established. Further, a technique involving Fourier Analysis was also developed to allow accurate interpretation of the resultant echo level in the system, as measured using the group delay test. This method permitted a realistic determination of the number of cases which required application of the filter techniques.

With the analysis and pre-installation evaluation tools developed from this system, it is now possible to recognize, analyze, and readily resolve this difficulty.

Acknowledgment

The success of this work was largely due to the support of Mr. Erkan Guciz whose many hours of explanations and guidance were invaluable. Mr. Harry Willems, Mr. Peter Nwafor, Mr. Ray Boyko, Mr. Greg Orseno, Mr. Roger Proulx and all of the Northern Telecom installation staff (who performed the very difficult field work) were also very strong contributors to this effort. Support provided by Mitec Electronics Ltd. (who developed the TE_{21} suppressive filter used in this application), Andrew Corporation, and Gabriel Electronics, all of whom worked with us to understand and correct the echoes in the system, was also invaluable.

References

[1] A.T. Schindler, "Minimization of envelope delay distortion due to mode conversions in circular waveguide and horn antenna systems," Northern Electric Co. Ltd. Research and Development Laboratories, June 1970.

[2] Milton A. Gerdine and H.F. Lenzing, "Reduction of delay distortion in a horn-reflector antenna system employing overmoded-waveguide feeder," *IEEE Trans. Commun. Technol.*, vol. Com-18, no. 1, Feb. 1970.

[3] P.A. Nwafor and M.C. Rochette, "TD-2M improvement program," *Bell Canada Rep.*, Radio Syst. Engineering.

[4] "A new microwave link analyzer for communications systems carrying up to 2700 telephone channels," *Hewlett Packard J.*, vol. 27, no. 3, Nov. 1975.

[5] Philip F. Panter, *Modulation, Noise, and Spectral Analysis Applied to Information Transmission.* New York: McGraw-Hill, 1965, pp, 288–292 and 370–373.

[6] C. M. Knop, E. Ostertag, and F. Willis, "Distortion in group delay ripple due to higher order mode reconversion in overmoded feeder waveguide," Andrew Corp., Orland Park, IL, Feb. 26, 1973.

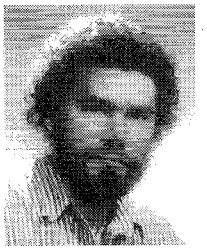

Rod Walker was born in Montreal, Quebec, Canada in June 1954. He received the Bachelor of Engineering degree in 1980 from McGill University.

From January 1980 to March 1985 he worked in the Communications Department of Canadian Pacific Rail. Since 1985 he has worked as a communications system engineer for Northern Telecom Inc. His experience has been in systems application work with VHF mobile radio (with Canadian Pacific) and in high capacity long haul fiber-optics and microwave radio systems.